CORROSION TESTS OF SS316H IN STATIC AND FLOWING U-BEARING FLUORIDE SALTS

Jaewoo Park[1], Qiufeng Yang[1], Jinsuo Zhang[1,*]
[1]Virginia Polytechnic Institution and State University, Blacksburg, VA, United States of America
*Email contact of corresponding author: zjinsuo5@vt.edu

Abstract
The purification of salt is indispensable to mitigate the corrosion of structural materials for molten salt reactors or other molten-salt applications. This study developed a salt-purification system to synthesize and purify NaF-KF-UF_4 salt (FUNaK) using Ar purging and hydrofluorination of impurities at high temperatures. Chronoamperometry (CA) was also used to remove metallic impurities in the hydrofluorinated FUNaK, and UF_3 was produced in the salt. This chemically purified FUNaK was used to study the corrosion of stainless steel 316H in static and flowing molten FUNaK to examine the effectiveness of salt purification on mitigating corrosion. Tests with the same conditions were also conducted with only thermally purified FUNaK for comparison. The results showed that the corrosion of SS316H by the chemically purified salt was significantly less than that by the thermally purified FUNaK.

1. Introduction

Hydrogen fluoride (HF), H_2O, oxides, and metallic impurities are main impurities that cause the corrosion of structural alloys for molten salt reactors (MSRs) [1,2]. HF reacts with metallic elements and produces corresponding fluorides and hydrogen gas [2]. H_2O is also a common impurity in salts due to their inherent hygroscopic nature [1]. H_2O reacts with metal fluorides and produces oxides and hydroxides with corrosive HF [3]. Dissolved oxides also can trigger reactions with metal fluorides and create the corresponding metal oxides [4]. When these reactions occur, insoluble metal oxides can be produced, as melting temperatures of the metal oxides tend to be higher than the melting temperature of the fluorides [4]. In addition, the oxides can contribute to the dissolution of metals into molten salt. Guo et al. reported that the formation of oxides on structural alloys might occur due to the oxidation of metals by dissolved oxygen ions [5]. These produced oxides might then be dissolved into molten salt [5]. Metallic impurities, such as FeF_2 and NiF_2 can also trigger the corrosion reactions which can be introduced to the salt during manufacture and storage of the salt [1,4].

Since impurities are detrimental to molten-salt systems, there have been many studies on the purification of salt. Oak Ridge National Laboratory developed a salt-purification system using a HF-H_2 treatment to remove oxides, hydroxides, sulfur, and structural-metal impurities from fluoride salts [2,6]. This HF-H_2 treatment was also used by Kelleher et al. to purify FLiBe salt [7]. In addition, it was suggested by Zhang et al. to add UF_3 in fluoride fuel salts, since it is thermodynamically more favorable for UF_3 to react with oxidants such as HF than the structural metals [8].

In this study, a salt-purification system was developed and fabricated to remove impurities in NaF-KF-UF_4 (FUNaK) salt using hydrofluorination and Ar purging. In addition, chronoamperometry (CA) was conducted to reduce metallic impurities in FUNaK introduced from the salt-purification system. Then, this chemically purified FUNaK (purified using hydrofluorination with CA) was used for static and dynamic corrosion tests. UF_3 was produced in the salt for a static corrosion test by dissolving U metal. In addition, other batches of FUNaK

with UF_3 were synthesized using only thermal purification. These salts were used for static and dynamic corrosion tests of stainless steel 316H (SS316H) to examine the effectiveness of salt purification on corrosion mitigation.

2. Experimental

Sodium fluoride (NaF, ≥99.0%, Sigma-Aldrich), potassium fluoride (KF, ≥99.5%, Sigma-Aldrich), and uranium tetrafluoride (UF_4, U is natural uranium, ≥85%, Cameco) were used to synthesize FUNaK. The metallic purities of these chemicals were confirmed using ICP-MS. The metallic purity of UF_4 purchased from Cameco was measured as 99.801 ± 0.038 wt% in this study. Non-metallic impurities of chemicals such as oxygen and hydrogen were also measured using combustion analysis and would be discussed in Section 3. The salt-purification system was used to synthesize and purify FUNaK. HF and Ar were used to purify the salt while it was being heated based on a heating schedule. The target temperatures of the schedule were selected based on temperatures for the dehydration of UF_4 and KF [9,10] and the hydrofluorination of UO_2 [11] reported or used by previous studies. The KHF_2 was used as a source of the HF gas [12], and the KHF_2 was heated at 623 K to produce HF gas. Metallic impurities introduced into the salt while it was being synthesized and purified using the salt-purification system were reduced by conducting CA. For the synthesis of thermally purified FUNaK, the individual salt components were heated in accordance with the heating schedule based on their dehydration temperatures. UF_3 was produced in chemically purified FUNaK for the static test and thermally purified FUNaK by dissolving U metal as given in Eq. (1). The U metal was hung by Ni wire and immersed in the salt at 973 K. Then, X-ray photoelectron spectroscopy was used to confirm the production of UF_3 in the salt.

$$\mathrm{U} + 3\mathrm{UF_4} \rightleftarrows 4\mathrm{UF_3} \tag{1}$$

Two static tests and two dynamic tests were conducted at 1073 K for 120 hours. The same ratio of specimen's surface to salt's mass (around 0.067 cm^2/g) was used for the static tests for comparison, and so as the dynamic tests (around 0.0067 cm^2/g). For the static tests, Ni wire was used to hang SS316H specimens. Boron nitride tubes were used to electrically isolate SS316H specimens with Ni wire from other experiment-setup components to prevent their galvanic effect on the corrosion of the specimens. For the dynamic tests, ring-shaped SS316H specimens fixed between BN tubes were spun at a rotating speed of 2 m/s. Glassy carbon crucibles were used to contain salts during static and dynamic corrosion tests. After the tests, surface and cross section of post-test specimens were analyzed using scanning electron microscopy with energy-dispersive X-ray spectroscopy (SEM/EDS) to study corrosion behaviors of SS316H.

3. Results and Discussion

Salt purification reduced concentrations of oxygen and hydrogen in salts. Table 1 shows concentrations of oxygen and hydrogen in as-received individual salt components before the purification process and FUNaK synthesized and purified using the salt-purification system. This indicates that oxygen and hydrogen in salts were removed by hydrofluorination and Ar purging. The oxygen content was reduced by converting oxides to fluorides using HF gas. In addition, the hydrogen content was reduced by removing moisture in the individual salts using their dehydration temperatures and Ar purging. Hydroxides might also exist in the salts, and

they are expected to be removed by their hydrofluorination. In addition, it was confirmed by using ICP-MS that concentrations of metallic impurities were reduced after conducting CA.

Table 1 Concentrations of oxygen and hydrogen in as-received NaF, KF, and UF_4 and purified FUNaK measured using combustion analysis

Salt	Concentration, μg/g	
	O	H
NaF	1608.26 ± 27.13	174.29 ± 8.15
KF	876.93 ± 94.10	48.92 ± 14.16
UF_4	1757.56 ± 156.28	37.02 ± 6.91
FUNaK	312.03 ± 123.85	15.12 ± 8.15

The static corrosion tests showed that the chemical purification reduced the corrosion of SS316H significantly. Fig. 1 shows backscattered electron (BSE) images for cross sections of SS316H specimens corroded by thermally purified FUNaK (Fig. 1a) and chemically purified FUNaK (Fig. 1b) with the EDS mapping result for the Cr distribution of Fig. 1b (Fig. 1c). The maximum depth of the grooves on the surface formed by the attack of the chemically purified FUNaK was around 7.24 μm. This depth is considerably smaller than the maximum attack depth of SS316H specimens corroded by thermally purified FUNaK (504.10 μm). Concentrations of corrosion products in post-test salt from the test using chemically purified was also much lower than those using thermally purified salt.

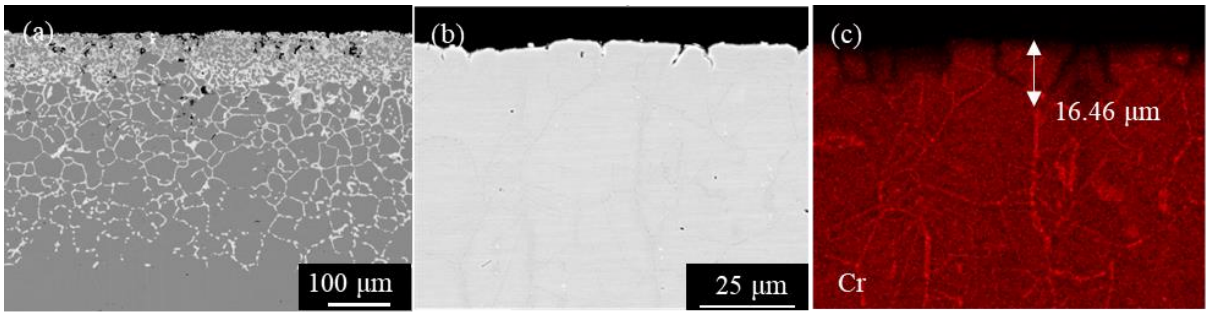

Fig. 1. BSE images of cross sections of SS316H specimens corroded by thermally purified FUNaK (a) and by chemically purified FUNaK (b) during static corrosion tests. Figure 1c represents the EDS mapping result for the Cr distribution of Figure 1b.

Fig. 1b shows grooves or pits at the surface of the specimen corroded by chemically purified FUNaK. The grooves were also observed along grain boundaries on the surface of the post-test specimen. This indicates that the dissolution of metallic elements from SS316H into FUNaK occurs more actively at grain boundaries than grains on the surface. The SS316H specimen corroded by chemically purified FUNaK showed the segregation of Cr at grain boundaries and Mo at grain boundaries and in grains. Fig. 1c displays that Cr was depleted at grain boundaries near the surface of the specimen more significantly than in grains. The maximum depth of the Cr depletion at the surface of the post-test specimen was around 16.46 μm. In addition, grooves formed on the surface are aligned with the grain boundaries depleted of Cr near the surface. This also indicates that the dissolution of metallic elements at the surface of SS316H occurs at grain boundaries more than grains. The Cr mapping results also show that Cr diffused to grain

boundaries from grains in the interior of the specimens and was segregated during corrosion tests.

The dynamic corrosion tests also showed that chemical purification significantly mitigated the corrosion of SS316H. Fig. 2 shows BSE images for cross sections of SS316H specimens corroded by thermally purified FUNaK (Fig. 2a) and chemically purified FUNaK (Fig. 2b). The maximum depth of salt attack by the chemically purified FUNaK was around 61.31 μm which is considerably smaller than the maximum attack depth of SS316H specimens corroded by thermally purified FUNaK (797.75 μm). However, some attack by the chemically purified FUNaK was still identified as shown in Fig. 2b, and pitting corrosion was observed on the surface of the post-test specimen. Same as the static corrosion tests, SS316H specimens from dynamic corrosion tests showed segregations of Cr and Mo in the bulk. In addition, it was observed from the dynamic test with thermally purified FUNaK that silver-colored layers were formed on the surface of the glassy carbon crucible where the salt contacted the crucible. The layers were identified mainly as $(Cr, Fe)_7C_3$ by using SEM/EDS and X-ray diffraction, and Cr-metal particles and dendrites concentrated with Fe and Cr were also observed. This indicates that dissimilar mass transfer occurred between SS316H and glassy carbon.

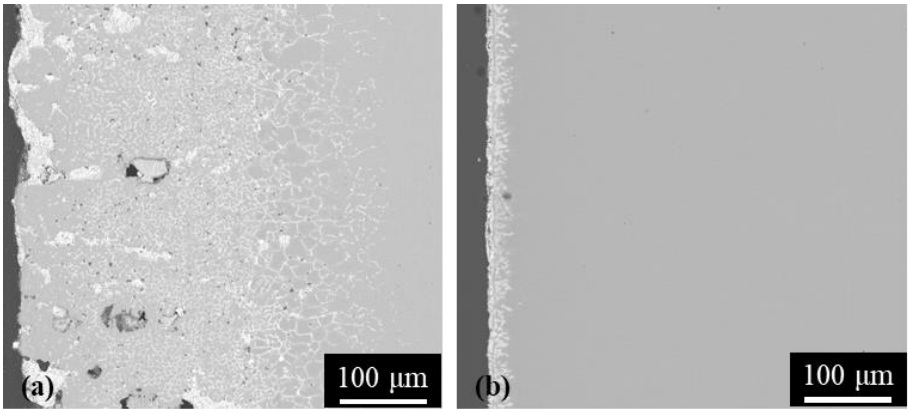

Fig. 2. BSE images of cross sections of SS316H specimens corroded by thermally purified FUNaK (a) and by chemically purified FUNaK (b) during dynamic corrosion tests.

Concentration changes of corrosion products in FUNaK were obtained using ICP-MS during the dynamic corrosion tests. It was observed that the concentration of Fe increased at the beginning of the tests and then decreased, while concentrations of Cr increased at the beginning of the tests and became steady. This indicates that the dissolved FeF_2 reacted with Cr of SS316H at the surface of specimens and accelerated the Cr depletion. The formation of Fe-concentrated layers on the surface of the post-test specimens was identified using SEM/EDS. These Fe-concentrated layers were also observed above Cr-depleted regions of specimens after static corrosion tests. The Cr concentration in FUNaK during the test with thermally purified salt decreased at the end of the test, which might be caused by the decrease in Cr dissolution from SS316H and the formation of $(Cr, Fe)_7C_3$.

4. Conclusion

This study developed a salt-purification system to reduce oxygen and hydrogen contents in salts and synthesize FUNaK. CA was conducted to reduce metallic impurities introduced into the purified FUNaK from the system. UF_3 was produced in FUNaK by using U metal. The chemically purified salts were used for static and dynamic corrosion tests to study the impact of salt purification on the corrosion of SS316H. Thermally purified FUNaK was also

synthesized and used for the corrosion tests with the same conditions for comparison. The corrosion of SS316H was significantly mitigated by chemically purifying salts. SS316H corroded by chemically purified salts showed much lower salt-attack depth and Cr depletion than those corroded by thermally purified FUNaK. The dissolution of corrosion products from SS316H in the chemically purified salt was also much lower than that in the thermally purified salt. The segregation of Cr at grain boundaries and Mo at grain boundaries and other areas in grains was observed for specimens after static and dynamic tests. For the static corrosion test with chemically purified FUNaK, grooves were formed along grain boundaries on the surface of the post-test specimen. These grooves were aligned with Cr-depleted and Cr-segregated grain boundaries in the bulk area of the specimen. For the dynamic corrosion test with chemically purified FUNaK, pitting corrosion was observed on the surface of the post-test specimen. The dynamic corrosion tests also indicated that Fe rapidly dissolved from SS316H into salt at the beginning of the tests, and the dissolved FeF_2 reacted with the Cr of SS316H resulting in the formation of Fe-concentrated layers on the surface of specimens. These Fe-concentrated layers were also observed on specimens used in static corrosion tests. $(Cr, Fe)_7C_3$ layers were formed on the surface of the glassy carbon crucible during the dynamic corrosion test using thermally purified FUNaK showing the occurrence of dissimilar mass transfer between SS316H and glassy carbon.

REFERENCES

[1] SRIDHARAN, K., ALLEN, T.R., "Corrosion in molten salts", Molten Salts Chemistry from Lab to Applications, Elsevier Inc., San Diego, California (2013).

[2] SHAFFER, J.H., "Preparation of MSRE fuel, coolant, and flush salts", Molten-Salt React. Progr. Semiannu. Prog. Rep. Period End. July 31, 1964, internal report, Oak Ridge National Laboratory, Oak Ridge, Tennessee, (1964) 288-303.

[3] PIZZINI, S., MORLOTTIE, R., Oxygen and hydrogen electrodes in molten fluorides, Electrochim. Acta. 10 (1965) 1033-1041.

[4] BAES, C.F., The chemistry and thermodynamics of molten salt reactor fuels, J. Nucl. Mater. 1 (1974) 149–162.

[5] GUO, S., ZHANG, J., WU, W., ZHOU, W., Corrosion in the molten fluoride and chloride salts and materials development for nuclear applications, Prog. Mater. Sci. 97 (2018) 448–487.

[6] SHAFFER, J.H., Preparing and Handling of Salt Mixtures for the Molten Salt Reactor Experiment, internal report, Oak Ridge National Laboratory, Oak Ridge, Tennessee, 1971.

[7] KELLEHER, B.C., DOLAN, K.P., BROOKS, P., ANDERSON, M.H., SRIDHARAN, K., Batch-scale hydrofluorination of $^7Li_2BeF_4$ to support molten salt reactor development, J. Nucl. Eng. Radiat. Sci. 1 (2015).

[8] ZHANG, J., FORSBERG, C.W., SIMPSON, M.F., GUO, S., LAM, S.T., SCARLAT, R.O., CAROTTI, F., CHAN, K.J., SINGH, P.M., DONIGER, W., SRIDHARAN, K., KEISER, J.R., Redox potential control in molten salt systems for corrosion mitigation, Corros. Sci. 144 (2018) 44–53.

[9] KATZ, J.J., SEABORG, G.T., The Chemistry of the Actinide and Transactinide Elements, 3rd ed., Springer, Dordrecht, The Netherlands, 2010.

[10] SHAMBERGER, P.J., REID, T., Thermophysical properties of potassium fluoride tetrahydrate from (243 to 348) K, J. Chem. Eng. Data. 58 (2013) 294–300.

[11] DELL, R.M., WHEELER, V.J., Chemical reactivity of uranium trioxide part 1.-conversion to U_3O_8, UO_2 and UF_4, Trans. Faraday Soc. (1962) 1590–1607.

[12] WESTRUM, E.F., PITZER, K.S., Thermodynamics of the system KHF_2-KF-HF, including heat capacities and entropies of KHF_2 and KF. The nature of the hydrogen bond in KHF_2, J. Am. Chem. Soc. 71 (1949) 1940–1949.